

Effects of Reaction Conditions on the Grafting Percentage of Poly(ethylene glycol)-*block*-poly(γ -benzyl *L*-glutamate)-*graft*-poly(ethylene glycol) Copolymer

Guo-quan Zhu,* Fa-gang Wang and Yu-ying Liu

School of Materials Science and Engineering, Shandong University of Technology,
Zibo 255049, People's Republic of China

No presente trabalho, o copolímero poli(etileno glicol)-*bloco*-poli-benzil *L*-glutamato)-*graft*-poli(etileno glicol) (PEG-*b*-PBLG-*g*-PEG) foi sintetizado pela reação de transesterificação do copolímero PEG-*bloco*-PBLG com a cadeia PEG. A estrutura e propriedades do copolímero PEG-*b*-PBLG-*g*-PEG foram investigadas por espectroscopia no infravermelho (FT-IR), microscopia de força atômica (AFM), microscopia eletrônica de varredura (SEM) e calorimetria diferencial de varredura (DSC). Foram investigados os efeitos de temperatura de reação, tempo de reação, e extensão da cadeia dos segmentos PBLG na porcentagem de enxerto do copolímero PEG-*b*-PBLG-*g*-PEG. Os resultados experimentais demonstraram que a porcentagem de enxerto do copolímero PEG-*b*-PBLG-*g*-PEG aumentou com o aumento do tempo e temperatura de reação, enquanto que o aumento do comprimento da cadeia de segmentos PBLG no copolímero bloco diminuiu a porcentagem de enxerto.

In the present work, poly(ethylene glycol)-*block*-poly(γ -benzyl *L*-glutamate)-*graft*-poly(ethylene glycol) (PEG-*b*-PBLG-*g*-PEG) copolymer was synthesized by the ester exchange reaction of PEG-*block*-PBLG copolymer with PEG chain. Structure and properties of PEG-*b*-PBLG-*g*-PEG copolymer were investigated by fourier transform infrared spectroscopy (FT-IR), atomic force microscopy (AFM), scanning electron microscopy (SEM), and differential scanning calorimeter (DSC). The effects of reaction temperature, reaction time, and the chain length of PBLG segments on the grafting percentage of PEG-*b*-PBLG-*g*-PEG copolymer were studied. Experimental results demonstrated that the grafting percentage of PEG-*b*-PBLG-*g*-PEG copolymer increased with the increase of both reaction temperature and reaction time, while the increase of the chain length of PBLG segments in block copolymer decreased the grafting percentage.

Keywords: effects, reaction condition, grafting percentage, morphology, poly(ethylene glycol)-*block*-poly(γ -benzyl *L*-glutamate)-*graft*-poly(ethylene glycol)

Introduction

It is well known that polypeptide science is a growing field of interest for both academic and commercial reasons.¹⁻¹² Because of the unique structures and properties, synthesized polypeptides and their copolymers have been investigated widely in the fields of protein simulation, macromolecular conformational study, catalysis, drug delivery, nanoreactors etc.¹³⁻²³

Recently, much interest has been focused on the self-association behavior of the copolymers composed of hydrophobic polypeptide segments and hydrophilic polymer chains.^{1,7-13} Cho *et al.*⁹ have reported the formation of polymeric micelles composed of poly(γ -benzyl

L-glutamate) and poly(ethylene oxide) in aqueous medium and the drug delivery system based on the core-shell nanoparticles with PBLG as the hydrophobic inner core and PEO as the hydrophilic outer shell. Kwon *et al.*¹³ reported that poly(β -benzyl *L*-aspartate) (PBLA)/poly(ethylene oxide) (PEO) diblock copolymers could self-assemble to form polymeric micelles composed of an outer shell of PEO and an inner core of PBLA in aqueous medium.

Relative to block and graft copolymers, polypeptide copolymers with both block and graft segments have received less attention. To our knowledge, few experimental works have been reported on the effects of reaction conditions on the grafting percentage of poly(ethylene glycol)-*block*-poly(γ -benzyl *L*-glutamate)-*graft*-poly(ethylene glycol) copolymer. In the present work, poly(ethylene glycol)-*block*-poly(γ -benzyl-*L*-glutamate)-*graft*-poly(ethylene

*e-mail: guoquanzhu888@163.com

glycol) copolymer has been synthesized. FT-IR, AFM, SEM, and DSC techniques were used to characterize the structure and property of PEG-*b*-PBLG-*g*-PEG copolymer. The effects of reaction temperature, reaction time, and the chain length of PBLG segments on the grafting percentage of PEG-*b*-PBLG-*g*-PEG copolymer were investigated.

Experimental

Materials

The amine-terminated α -methoxy- ω -amino poly(ethylene glycol) (AT-PEG, MW = 5000 g mol⁻¹) and poly(ethylene glycol methyl ether) (mPEG, MW = 350 g mol⁻¹) were purchased from Sigma Inc., and used without further purification. Hexane, tetrahydrofuran (THF) and 1,4-dioxane are of analytical grade and dried with sodium before use. All other solvents are of analytical grade and used without further purification.

Syntheses of polypeptide homopolymer and copolymers

The PBLG sample was prepared by a standard *N*-carboxyl- γ -benzyl-*L*-glutamate anhydride (NCA) method.¹⁷⁻¹⁹ The molecular weight of PBLG was estimated from the intrinsic viscosity measured in dichloroacetic acid (DCA).²⁴ The molecular weight of PBLG homopolymer used in the study is 50000.

PBLG-*block*-PEG copolymer (shown in Figure 1a) was obtained by the ring-opening polymerization of γ -BLG NCA initiated by AT-PEG (MW = 5000 g mol⁻¹) in 1,4-dioxane at room temperature for 72 h.^{1,19} PEG-*b*-PBLG-*g*-PEG copolymer (shown by Figure 1b) was obtained by the ester exchange reaction of PBLG-*block*-PEG with mPEG (MW = 350 g mol⁻¹) in 1,2-dichloroethane with *p*-toluenesulfonic acid as a catalyst according to the method described in references.^{1,19} In the grafting reaction, the mole ratio of mPEG to PBLG segments is (20-30):1, the weight ratio of catalyst to PBLG segments is 5:1, PBLG/dichloroethane is 1 g/200 mL, and the reaction temperature is controlled between 55 - 60 °C with a precision of ± 0.1 °C. The pure PEG-*b*-PBLG-*g*-PEG copolymer was obtained by dialysis. Briefly, the polymer solution was concentrated and then dialyzed against deionized water using dialysis membrane (3500 molecular weight cut-off) to remove the mPEG and the organic solvents for 72 h at room temperature. It was preferred that the deionized water was exchanged at intervals of 4 - 5 h. The wet copolymer was dried by freeze-drying method. The molecular weights of PBLG-*block*-PEG copolymers and the grafting percentage of PEG-*b*-PBLG-*g*-PEG copolymer were estimated by nuclear magnetic resonance (NMR) measurements (Avance 550). It was calculated by the peak intensities of the methylene proton signal (5.11 ppm) of polypeptide and the ethylene proton signal (3.64 ppm) of PEG in the ¹H NMR spectrum.^{1,19,25} To emphasize one point, the

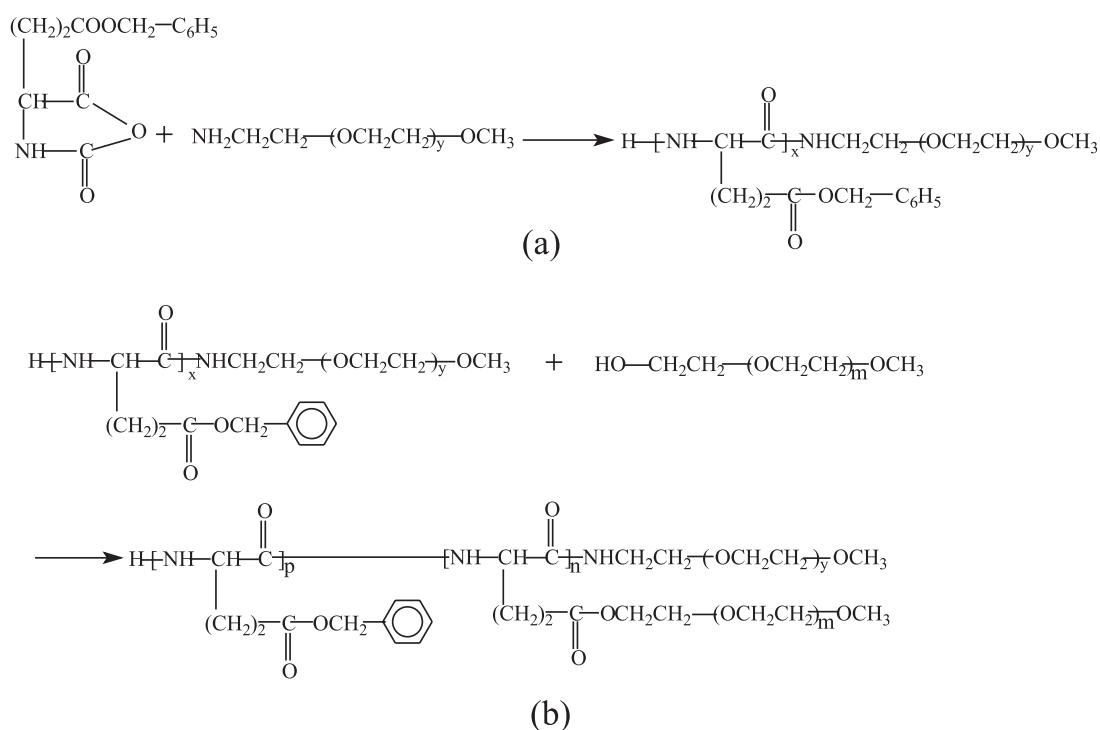


Figure 1. Syntheses of (a) PBLG-*block*-PEG and (b) PEG-*b*-PBLG-*g*-PEG.

peak area (A) used in calculating the grafting percentage of PEG-*b*-PBLG-*g*-PEG is the subtraction of A_1 and A_2 ($A_1 > A_2$), where A_1 is the peak area (3.64 ppm) in PEG-*b*-PBLG-*g*-PEG spectrum, A_2 is the peak area (3.64 ppm) in PBLG-*block*-PEG spectrum.²⁵ According to the NMR analysis, the molecular weights of PBLG-*block*-PEG copolymers are 63000, 77000, and 98000, respectively, and the corresponding PEG-*b*-PBLG-*g*-PEG copolymers synthesized were denoted as PEG-*b*-PBLG-*g*-PEG1 (*ab.* EGE(*bg*)1), PEG-*b*-PBLG-*g*-PEG2 (*ab.* EGE(*bg*)2), and PEG-*b*-PBLG-*g*-PEG3 (*ab.* EGE(*bg*)3), respectively. The structural representation of PEG-*b*-PBLG-*g*-PEG copolymer is shown in Figure 2.

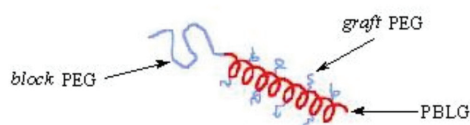


Figure 2. Structural representation of PEG-*b*-PBLG-*g*-PEG copolymer.

FT-IR analysis

FT-IR spectra of PBLG homopolymer and PEG-*b*-PBLG-*g*-PEG copolymer samples were measured on a Nicolet 5700 FT-IR spectrometer between 4,000 and 400 cm^{-1} .

AFM measurements

Polypeptide copolymer specimens were prepared by casting films from 30% polypeptide copolymer solution in

chloroform onto clean glass plates and drying them under vacuum at 50 °C. The surface morphology of polypeptide copolymer films was characterized on a Nanoscope IIIA Multimode AFM instrument (Digital Instruments, Inc., USA) in air at ambient conditions using tapping mode probes with constant amplitude (200 mV).

SEM photomicrographs

Gold was sprayed on samples in vacuum. Investigation was carried out using a scanning electron microscope (Sirin 200, FEI, Holland). Accelerating voltage was 10 kV and photographs of cross-section of PBLG homopolymer and PEG-*b*-PBLG-*g*-PEG were taken.

DSC analysis

DSC measurements were made on a DSC Q100 differential scanning calorimeter, the temperature calibrated with indium in nitrogen atmosphere. About 7 mg sample was weighted very accurately. The temperature was controlled within the range between 100 °C and 400 °C, the heating rate was 20 °C min^{-1} .

Results and Discussion

FT-IR studies

Curves a, b, and c in Figure 3 present the FT-IR spectra of PEG-*b*-PBLG-*g*-PEG1 (*ab.* EGE(*bg*)1), PBLG homopolymer, and their subtraction (*ab.* EGE(*bg*)1-PBLG), respectively, where spectrum c is obtained from spectra a

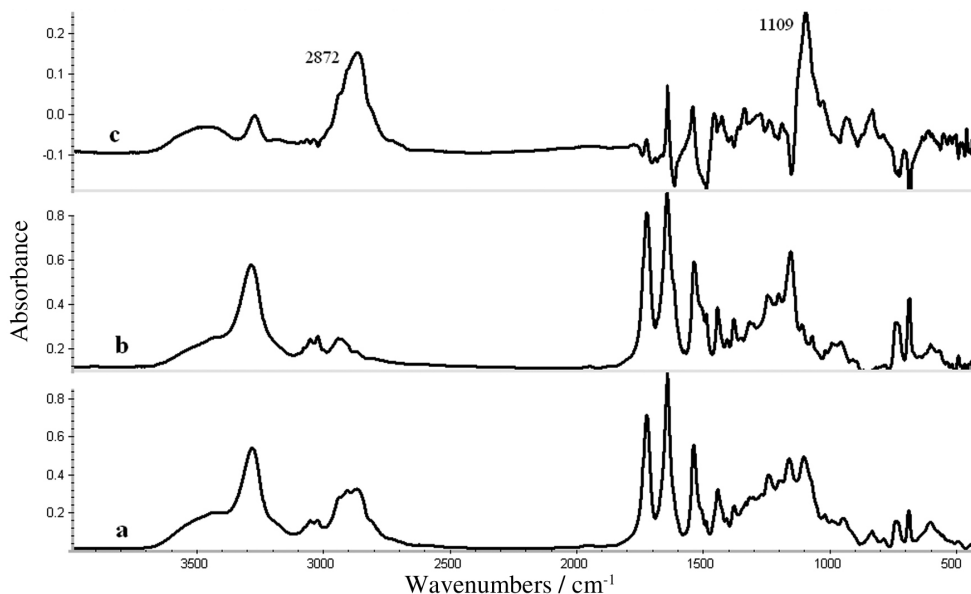


Figure 3. FT-IR spectra of (a) PEG-*b*-PBLG-*g*-PEG1 (*ab.* EGE(*bg*)1), (b) PBLG homopolymer, and (c) EGE(*bg*)1-PBLG (their subtraction).

and b. As it can be seen from Figure 3, the peak appearing at 1732 cm^{-1} (corresponding to C=O stretching band of the ester group in the side chain), the peak at 3287 cm^{-1} (corresponding to N-H stretching vibration in main chain), the peak at 1654 cm^{-1} (corresponding to the α -helix amide I band), the peak at 1548 cm^{-1} (corresponding to the α -helix amide II band) are detected in spectra a and b. This phenomenon demonstrates that both PBLG homopolymer and PEG-*b*-PBLG-*g*-PEG1 copolymer contain PBLG segments in α -helix structure.^{26,27} As seen from spectrum c, the peaks appearing at 1109 cm^{-1} and 2872 cm^{-1} can be assigned to C-O-C stretching band and C-H stretching band of PEG segments, respectively.²⁷ This situation proves that PEG segments also exist in PEG-*b*-PBLG-*g*-PEG1 copolymer.

AFM measurements

As is known, the AFM image indicated the surface hardness of polymers. Figure 4 presents the AFM phase images of (a) PBLG homopolymer film surface, and (b) PEG-*b*-PBLG-*g*-PEG1 copolymer film surface. As it can be seen from Figure 4a, the phase image of PBLG

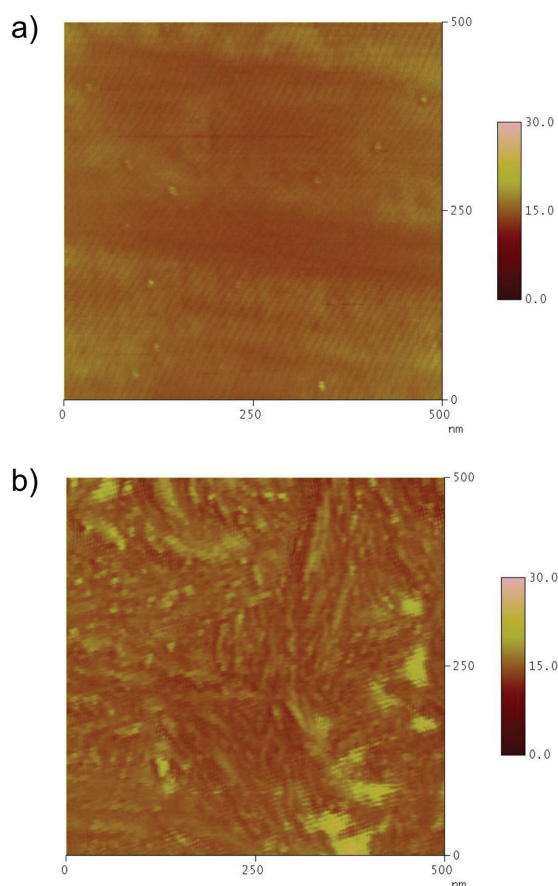


Figure 4. AFM phase images of (a) PBLG homopolymer, and (b) PEG-*b*-PBLG-*g*-PEG1 copolymer.

homopolymer film surface showed single darker color responding to the same hardness, indicating PBLG homopolymer was composed of only PBLG segments.^{28,29} Also seen from Figure 4b, the phase image of PEG-*b*-PBLG-*g*-PEG1 copolymer film surface showed both brighter parts and darker parts. As described in previous documents,^{30,31} the darker parts responded to the hard PBLG phase, while the brighter parts responded to the soft PEG phase. This phenomenon verified that PEG-*b*-PBLG-*g*-PEG copolymer was composed of both PBLG segments and PEG segments.

SEM studies

The microstructural morphologies of PBLG homopolymer and PEG-*b*-PBLG-*g*-PEG copolymer were evaluated by scanning electron microscopy. Figures 5a and 5b show the photographs of cross-section of PBLG homopolymer and PEG-*b*-PBLG-*g*-PEG1, respectively. As shown in Figure 5, the internal microstructure of PEG-*b*-PBLG-*g*-PEG1 copolymer is much different from that of PBLG homopolymer. The internal microstructure of PBLG homopolymer is a rather rough surface, which is caused by the rigid PBLG segments with α -helix structure.³²

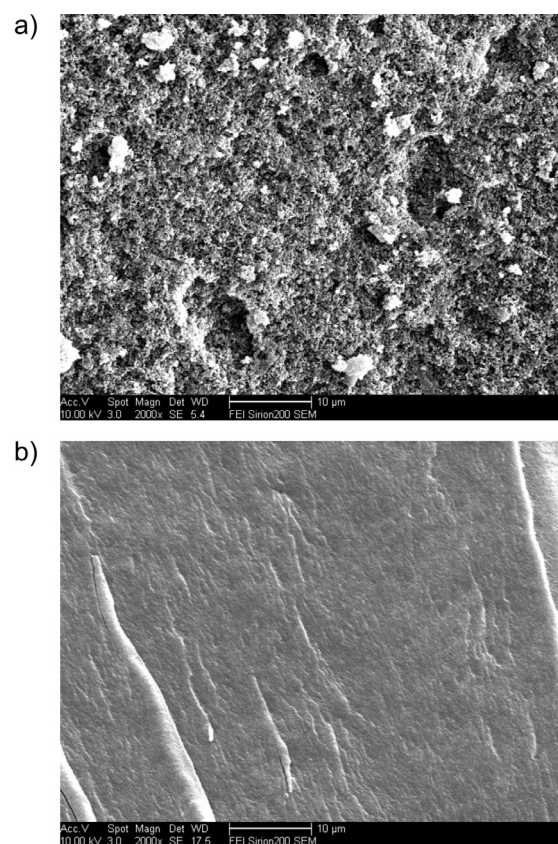


Figure 5. SEM photographs of cross-section of (a) PBLG homopolymer, and (b) PEG-*b*-PBLG-*g*-PEG1 copolymer (magnification 2000 \times).

The internal microstructure of PEG-*b*-PBLG-*g*-PEG1 copolymer is a relatively smooth surface, which is caused by the interaction and the better compatibility between the rigid PBLG segments and the soft PEG segments composed of (CH₂CH₂O) structural units, suggesting the change of the internal microstructure of PEG-*b*-PBLG-*g*-PEG1 copolymer could be attributed to the introduction of soft PEG chains.

DSC analysis

DSC curves of PBLG homopolymer (shown as curve a) and PEG-*b*-PBLG-*g*-PEG1 copolymer (shown as curve b) are presented in Figure 6. By comparing curve a with curve b, it is found that the melting point of PBLG segments in PEG-*b*-PBLG-*g*-PEG1 copolymer becomes lower than that of PBLG homopolymer.¹⁰ As mentioned above, the soft PEG segments composed of (CH₂CH₂O) structural units hold better compatibility with PBLG segments in PEG-*b*-PBLG-*g*-PEG1 copolymer, indicating the introduction of PEG segments debases the melting point of PBLG segments in PEG-*b*-PBLG-*g*-PEG1 copolymer.

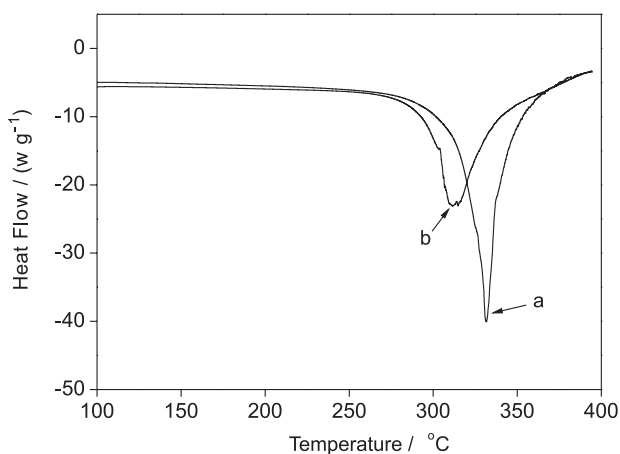


Figure 6. DSC curves of (a) PBLG homopolymer and (b) PEG-*b*-PBLG-*g*-PEG1.

Effects of reaction temperature on the grafting percentage of PEG-*b*-PBLG-*g*-PEG copolymer

Table 1 shows the effects of the reaction temperature on the grafting percentage of PEG-*b*-PBLG-*g*-PEG1, where the reaction time is 72 h. As seen from Table 1, the grafting percentage of PEG-*b*-PBLG-*g*-PEG1 increases with the augment of reaction temperature. As noted, the ester exchange reaction is a reversible reaction; under the same reaction conditions, the elevation of reaction temperature promotes the positive reaction and, as a result, the grafting percentage increases. To avoid the decomposition of

Table 1. The effects of the reaction temperature on the grafting percentage of PEG-*b*-PBLG-*g*-PEG1^a

Reaction temperature (°C)	Grafting percentage (%)
55	23.2
58	26.1
60	28.3

^aThe reaction time is 72 h.

polypeptide segments, the reaction temperature is usually kept under 60 °C.

Effects of reaction time on the grafting percentage of PEG-*b*-PBLG-*g*-PEG copolymer

Table 2 presents the effects of the reaction time on the grafting percentage of PEG-*b*-PBLG-*g*-PEG1, where the reaction temperature is 55 °C. As is shown in Table 2, the grafting percentage of PEG-*b*-PBLG-*g*-PEG1 increases with the increase of reaction time, and the increasing degree of grafting percentage gradually debases with the augment of reaction time. As mentioned above, the ester exchange reaction is a reversible process, and the reaction degree depends on the reactant ratio and catalyst, among other variables. At the reaction onset, mPEG is superfluous, and the positive reaction is faster than negative reaction. This phenomenon indicates the increase of grafting percentage with increasing reaction time. Due to product accumulation, the reaction speed gradually slows down. Accordingly, the increasing degree of grafting percentage gently decreases.

Table 2. The effects of the reaction time on the grafting percentage of PEG-*b*-PBLG-*g*-PEG1^a

Reaction time (h)	Grafting percentage (%)
24	11.5
48	20.4
72	23.2

^aThe reaction temperature is 55 °C.

Effects of the chain length of PBLG segments in block copolymer on the grafting percentage of PEG-*b*-PBLG-*g*-PEG copolymer

Table 3 presents the effects of the chain length of PBLG segments on the grafting percentage of PEG-*b*-PBLG-*g*-PEG copolymer, where the reaction temperature is 55 °C, the reaction time is 72 h. As shown in Table 3, the grafting percentage of copolymer decreases with the increase of the chain length of PBLG segments. As known, under the same reaction conditions, the longer the PBLG segments in block

Table 3. The effects of the chain length of PBLG segments in block copolymer on the grafting percentage of PEG-*b*-PBLG-*g*-PEG^a

Sample	MW of PBLG segments (g mol ⁻¹)	Grafting percentage (%)
EGE(<i>bg</i>)1	58 000	23.2
EGE(<i>bg</i>)2	72 000	21.1
EGE(<i>bg</i>)3	93 000	17.8

^aThe reaction temperature is 55 °C, the reaction time is 72 h.

copolymer, the stronger the intermolecular entanglement, and the lower the reaction speed. This phenomenon reveals the decrease of the grafting percentage with increasing the chain length of PBLG segments in block copolymer.

Conclusions

Poly(ethylene glycol)-*block*-poly(γ -benzyl *L*-glutamate)-*graft*-poly(ethylene glycol) copolymer has been synthesized. FT-IR and AFM analysis proved that PEG-*b*-PBLG-*g*-PEG copolymer is composed of both PEG and PBLG segments. SEM photographs demonstrated that the introduction of PEG segments changed the microstructure of PBLG segments in PEG-*b*-PBLG-*g*-PEG copolymer. DSC data testified that the introduction of PEG segments decreased the melting point of PBLG segments in PEG-*b*-PBLG-*g*-PEG copolymer. Experimental results verified that, at the same reaction conditions, the grafting percentage of PEG-*b*-PBLG-*g*-PEG copolymer increased with the augment of both reaction temperature and reaction time, while the increase of the chain length of PBLG segments in block copolymer decreased the grafting percentage.

Acknowledgements

This work is supported by the Natural Science Foundation of Shandong Province (No. ZR2009FL019).

References

1. Tang, D. M.; Lin, J. P.; Lin, S. L.; Zhang, S. N.; Chen, T.; Tian, X. H.; *Macromol. Rapid Commun.* **2004**, *25*, 1241.
2. Gao, Z. S.; Desjardins, A.; Eisenberg, A.; *Macromolecules* **1992**, *25*, 1300.
3. Lin, J. P.; Zhu, J. Q.; Chen, T.; Lin, S. L.; Cai, C. H.; Zhang, L. S.; Zhuang, Y.; Wang, X. S.; *Biomaterials* **2009**, *30*, 108.
4. Lin, J. P.; Zhang, S. N.; Chen, T.; Liu, C. S.; Lin, S. L.; Tian, X. H.; *J. Biomed. Mater. Res., Part B* **2006**, *76B*, 432.
5. Zhong, X. F.; Varshney, S. K.; Eisenberg, A.; *Macromolecules* **1992**, *25*, 7160.

6. Moffitt, M.; Eisenberg, A.; *Macromolecules* **1997**, *30*, 4363.
7. Harada, A.; Cammas, S.; Kataoka, K.; *Macromolecules* **1996**, *29*, 6183.
8. Cho, C. S.; Cheon, J. B.; Jeong, Y. I.; Kim, I. S.; Kim, S. H.; Akaike, T.; *Macromol. Rapid Commun.* **1997**, *18*, 361.
9. Cho, C. S.; Nah, J. W.; Jeong, Y. I.; Cheon, J. B.; Asayama, S.; Ise, H.; Akaike, T.; *Polymer* **1999**, *40*, 6769.
10. Oh, I.; Lee, K.; Kwon, H. Y.; Lee, Y. B.; Shin, S. C.; Cho, C. S.; Kim, C. K.; *Int. J. Pharm.* **1999**, *181*, 107.
11. Markland, P.; Amidon, G. L.; Yang, V. C.; *Int. J. Pharm.* **1999**, *178*, 183.
12. Jeong, Y. I.; Nah, J. W.; Lee, H. C.; Kim, S. H.; Cho, C. S.; *Int. J. Pharm.* **1999**, *188*, 49.
13. Kwon, G.; Naito, M.; Yokoyama, M.; Okano, T.; Sakurai, Y.; Kataoka, K.; *Langmuir* **1993**, *9*, 945.
14. Cheon, J. B.; Jeong, Y. I.; Cho, C. S.; *Polymer* **1999**, *40*, 2041.
15. Inomata, K.; Ohara, N.; Shimizu, H.; Nose, T.; *Polymer* **1998**, *39*, 3379.
16. Harada, A.; Kataoka, K.; *Macromolecules* **1995**, *28*, 5294.
17. Lin, J. P.; Liu, N.; Chen, T.; Zhou, D. F.; *Polymer* **2000**, *41*, 6189.
18. Lin, J. P.; Abe, A.; Furuya, H.; Okamoto, S.; *Macromolecules* **1996**, *29*, 2584.
19. Li, T.; Lin, J. P.; Chen, T.; Zhang, S. N.; *Polymer* **2006**, *47*, 4485.
20. Lin, J. P.; Zhang, S. N.; Chen, T.; Lin, S. L.; Jin, H. T. *Int. J. Pharm.* **2007**, *336*, 49.
21. Lin, J. P.; Zhu, G. Q.; Zhu, X. M.; Lin, S. L.; Nose, T.; Ding, W. W.; *Polymer* **2008**, *49*, 1132.
22. Chen, T.; Lin, S. L.; Lin, J. P.; Zhang, L. S.; *Polymer* **2007**, *48*, 2056.
23. Liu, N.; Lin, J. P.; Chen, T.; Chen, J. D.; Zhou, D. F.; Li, L.; *Polym. J.* **2001**, *33*, 898.
24. Abe, A.; Yamazaki, T.; *Macromolecules* **1989**, *22*, 2138.
25. Zhu, G. Q.; *J. Macromol. Sci., Part A: Pure Appl. Chem.* **2009**, *46*, 892.
26. Higashi, N.; Kawahara, J.; Niwa, M.; *J. Colloid Interface Sci.* **2005**, *288*, 83.
27. Wang, Q. M.; Teng, W.; Zhang, J. X.; Pan, S. R.; *Chin. J. Appl. Chem.* **2006**, *23*, 965.
28. Ibarboure, E.; Papon, E.; Rodriguez-Hernandez, J.; *Polymer* **2007**, *48*, 3717.
29. Lee, N. H.; Frank, C. W.; *Polymer* **2002**, *43*, 6255.
30. Minich, E. A.; Nowak, A. P.; Deming, T. J.; *Polymer* **2004**, *45*, 1951.
31. Park, Y.; Choi, Y.-W.; Park, S.; Cho, C. S.; Fasolka, M. J.; Sohn, D.; *J. Colloid Interface Sci.* **2005**, *283*, 322.
32. Cho, C. S.; Jeong, Y. I.; Kim, S. H.; Nah, J. W.; Kubota, M.; Komoto, T.; *Polymer* **2000**, *41*, 5185.

Received: June 22, 2009

Web Release Date: December 30, 2009